Physical properties of high-entropy alloys

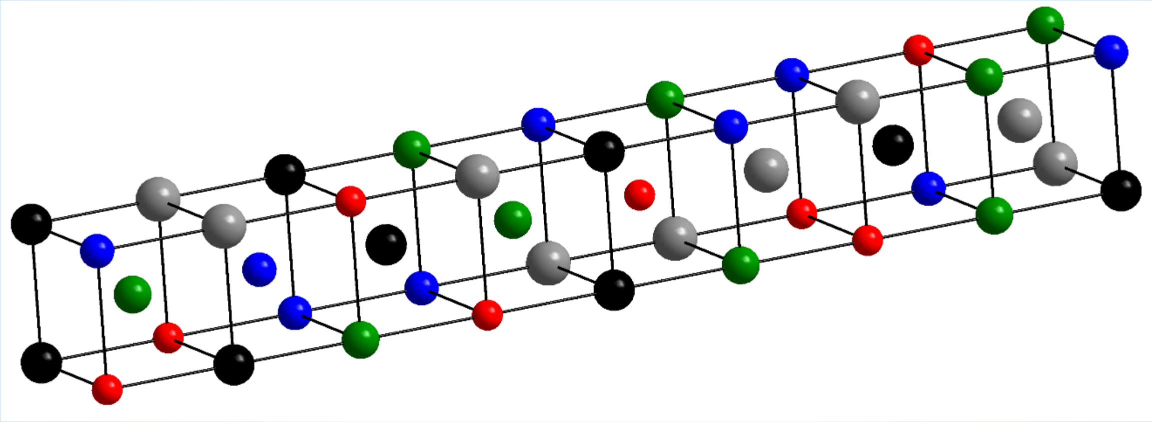

Janez Dolinšek

Institut "Jožef Stefan", Ljubljana, Slovenija

University of Ljubljana
Faculty of Mathematics and Physics

Traditional metallic alloy systems

- based on one principal chemical element as the matrix,

- **other elements incorporated in small amounts for property/processing enhancement,**

- **about 30 practical alloy systems developed (Fe (steels), Al, Cu, Ti, Mg, Ni-based).**

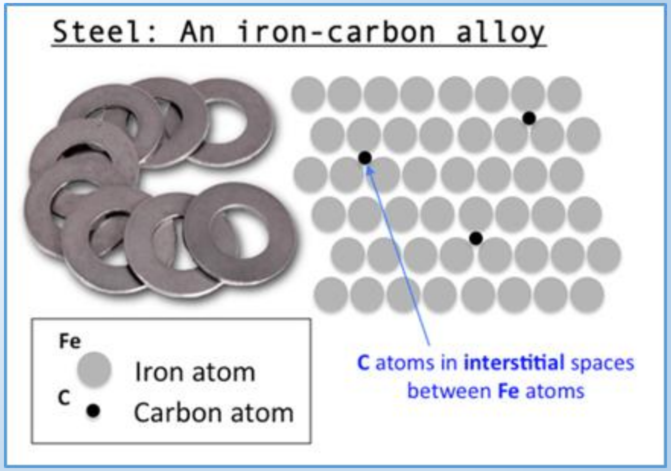

Alloys with more than one principal element

Intermetallic compounds (structurally simple or complex - CMAs)

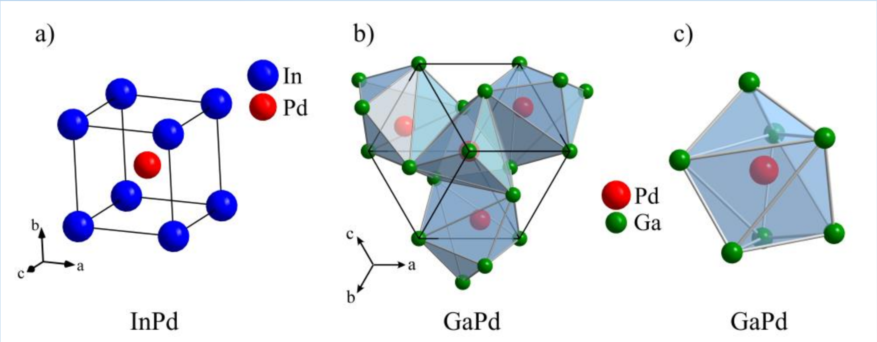

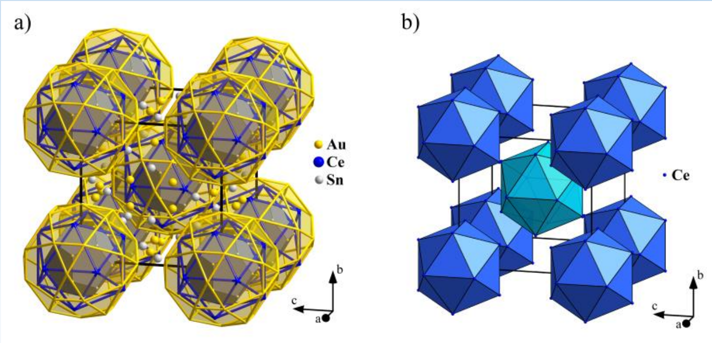

$Gd_3Au_{13}Sn_4$

Bulk amorphous alloys (metallic glasses, Pd, Ln, Zr, Fe, Mg-based)

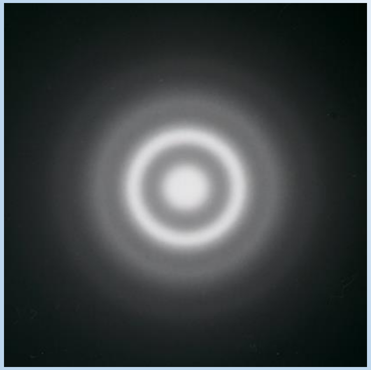

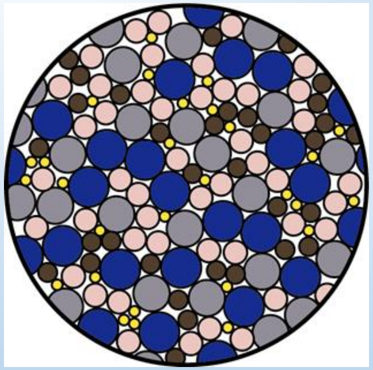

$Zr_{69.5}Cu_{12}Ni_{11}Al_{7.5}$ XRD pattern

Alloys with more than one principal element

Quasicrystals

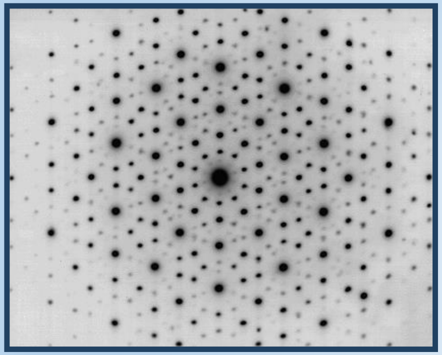

diffraction pattern

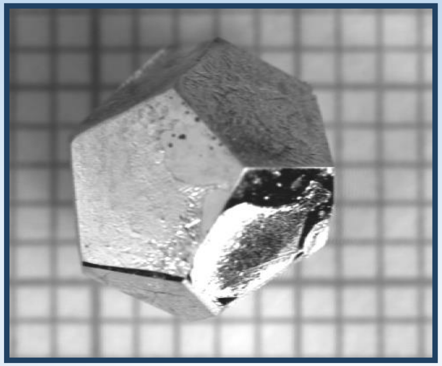

icosahedral Mg-Zn-Dy

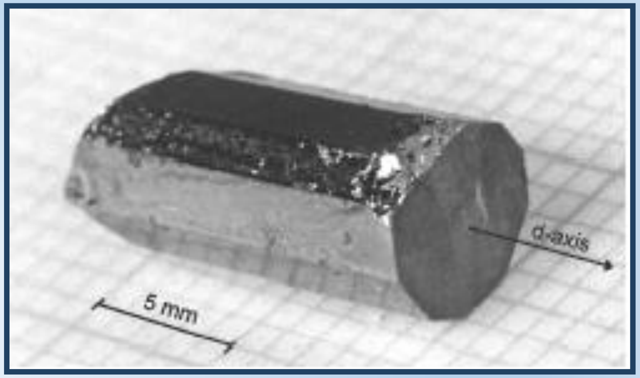

decagonal Al-Ni-Co

"forbidden" symmetries: 5-, 8-, 10-, 12-fold axes

Shechtman *et al.*, Phys. Rev. Lett. 53, 1951 (1984)

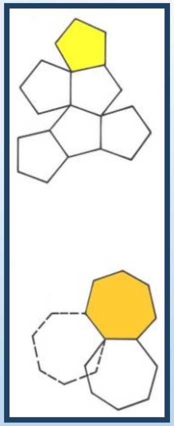

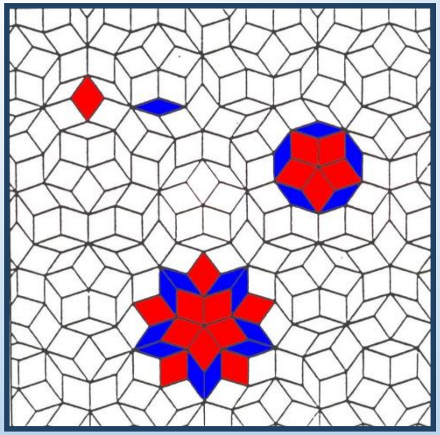

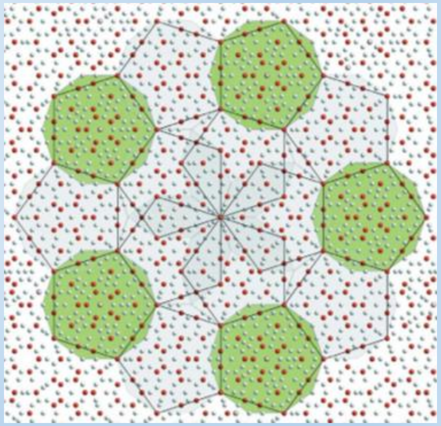

High-Entropy Alloys (HEAs)

- **new concept of alloy design with multiple principal elements in near-equimolar ratios,**
- **high entropy of mixing can stabilize disordered solid-solution phases with simple structures (bcc, fcc, hcp) and small unit cells,**
- **topologically ordered lattice with exceedingly high chemical (substitutional) disorder.**

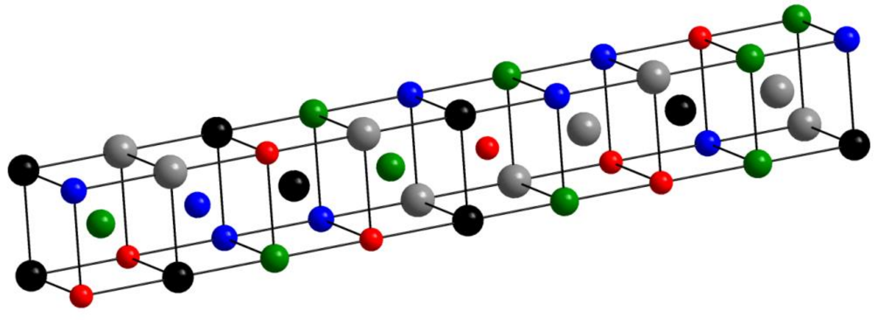

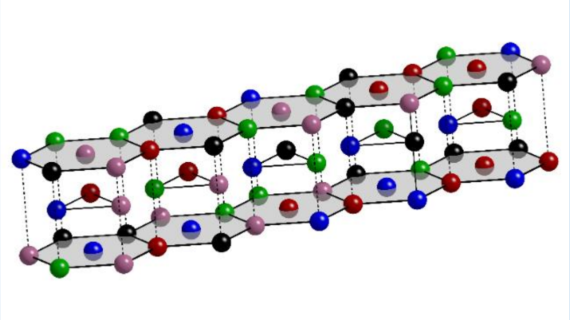

HEA: ***"metallic glass on a simple, ordered lattice"***

J.W. Yeh, *et al,* Adv. Eng. Matter. 6, 299 (2004),
J.W. Yeh, Ann. Chim. Sci. Mat. 31, 633 (2006).

High-Entropy Alloys (HEAs)

Conditions for the HEA-phase formation:

- high entropy of mixing should be achieved,

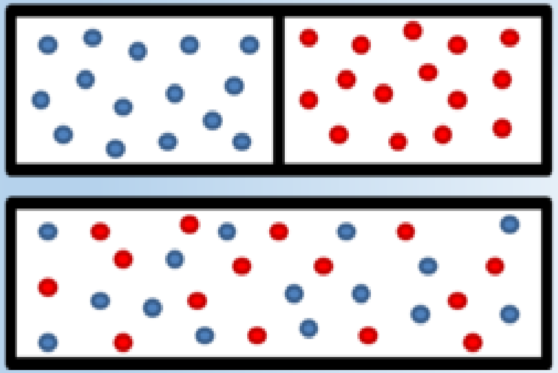

random mixing of ideal gasses

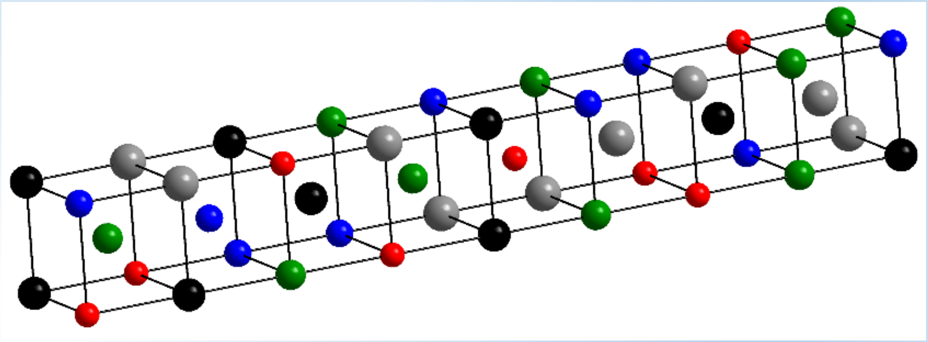

random mixing in a solid solution

- alloy must be composed of 5 or more majority elements in similar concentrations (from 5 to 35 at. % for each element),

- no element should exceed 50 at. % concentration.

HEA phase stabilization

- **minimization of Gibbs free energy** $G = H - TS$ **by the entropic term**

- **mixing free energy:** $\Delta G_{mix} = \Delta H_{mix} - T\Delta S_{mix}$

- **mixing (configurational) entropy of an *r*-element ideal gas (** $\Delta H_{mix} = 0$ **):**

$$\Delta S_{mix} = -nR\sum_{i=1}^{r} x_i \ln x_i$$

$x_i = n_i / n$ ... molar fraction of component *i*

- **equimolar concentrations of elements:** $x_i = 1/r$

→ **entropy of mixing reaches maximum** $\Delta S_{mix} = nR\ln r$

HEA phase stabilization

mixing entropy versus the number of elements in equimolar alloys

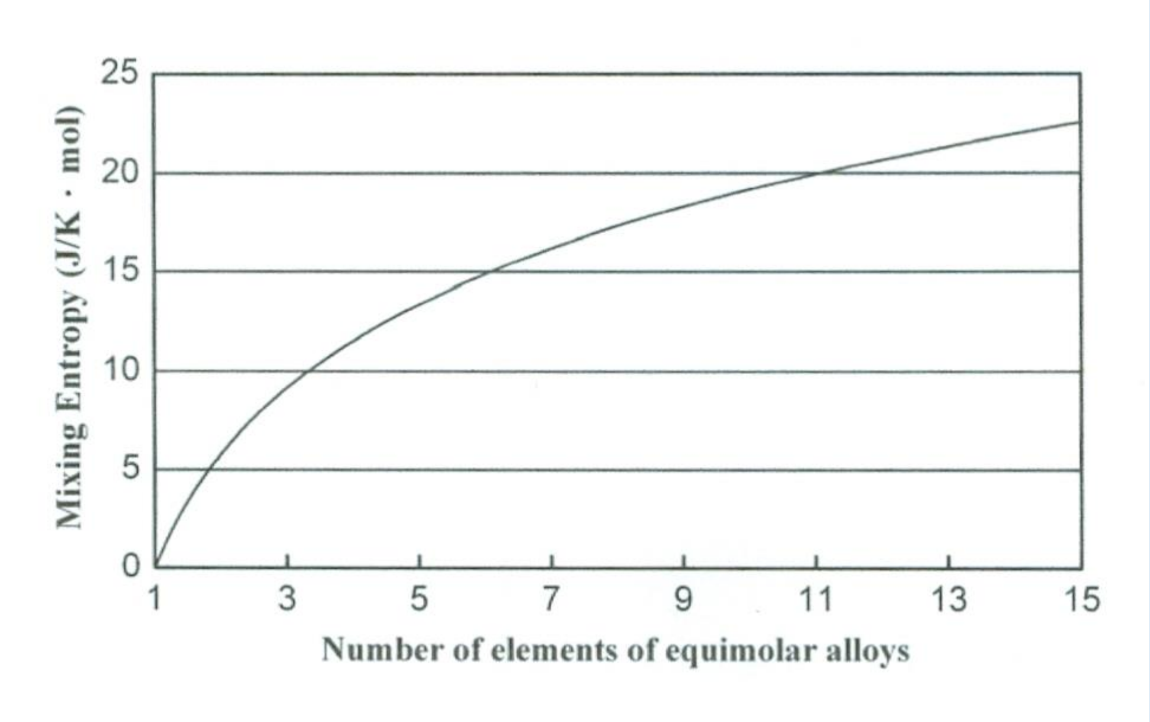

J.-W. Yeh, Annales De Chimie – Science des Materiaux 31, 633 (2006)

HEA phase stabilization - example

- five-component mixture (*r* = 5) with equimolar ratios of the elements:

$$\Delta S_{mix} = R \ln 5 = 13.4\ J/molK$$

- **high temperature, e.g., T = 2000 K:**

$$T\Delta S_{mix} = 26.8\ kJ/mol$$

energy gain of a few 10 kJ/mol is enough for the entropic stabilization of a disordered solid-solution phase with a simple structure (bcc, fcc, hcp), in competition with ordered complex crystalline intermetallic phases

HEA phase stability – ideal solid solutions

Ideal solutions:

- interactions between every pair of molecular kinds are the same,

$$\Delta H_{mix} = 0$$

$$\Delta G_{mix} = -T\Delta S_{mix}$$

- **mixing of the elements is completely random,**

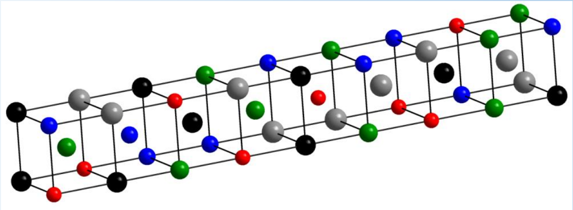

- solid solution with a simple structure is stabilized by the entropy term and is thermodynamically stable down to low temperatures.

Examples of ideal solid solutions: Mixtures of rare-earth elements

the system Gd-Tb-Dy-Ho-Er-Tm-Lu + Ce

heavy RE (Gd-Tb-Dy-Ho-Er-Tm-Lu) light RE (Ce)

Tb-Dy-Ho-Er-Tm

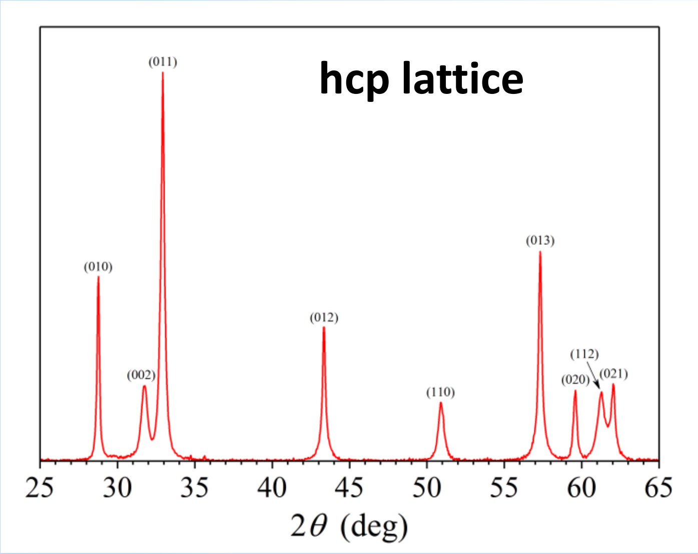

XRD

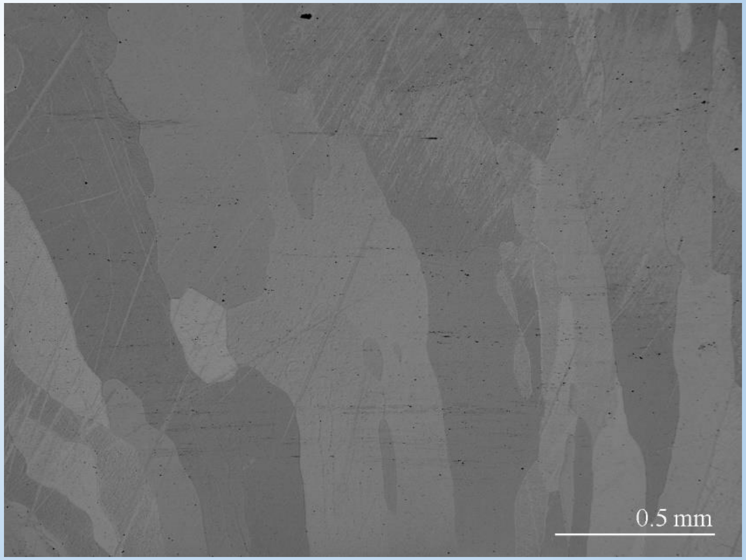

SEM BSE

HEA phase stability – regular solid solutions

- real solid solution ($\Delta H_{mix} \neq 0$): interactions between different molecular kinds are different,

- low temperatures: the entropy term $T\Delta S_{mix}$ becomes too small to stabilize a HEA phase,

- sluggish atomic diffusion in multi-component mixtures hinders phase transformations
→ simple high-*T* structure quenched down to low-*T* (metastable),

$\Delta H_{mix} < 0$: intermetallic phases precipitate at the nm scale,

$\Delta H_{mix} > 0$: phase separation (dendrites).

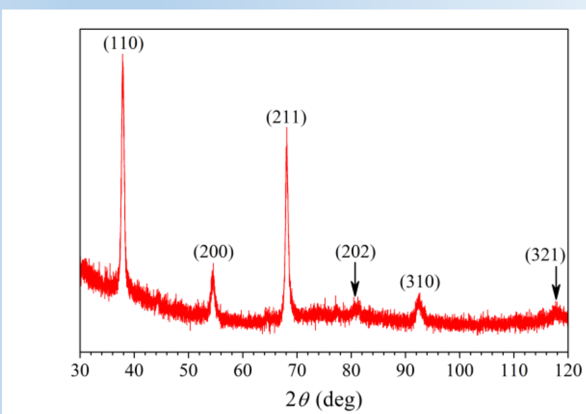

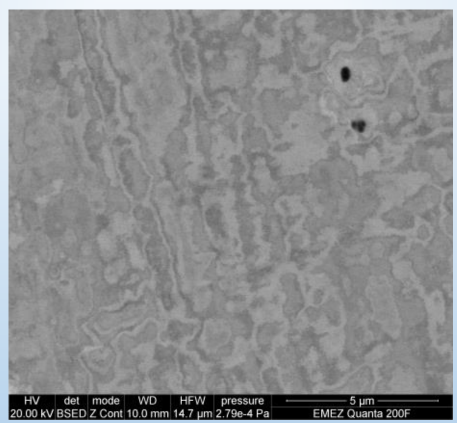

$Ta_{34}Nb_{33}Hf_8Zr_{14}Ti_{11}$ bcc HEA

SEM BSE image at the µm scale

$CoCrFeNiZr_{0.45}$ bcc HEA - regular solid solution

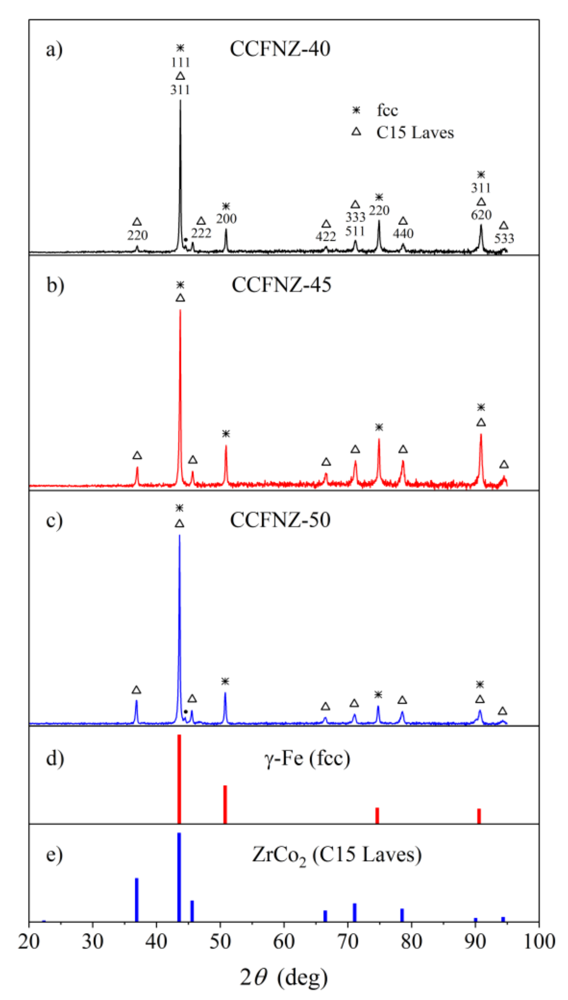

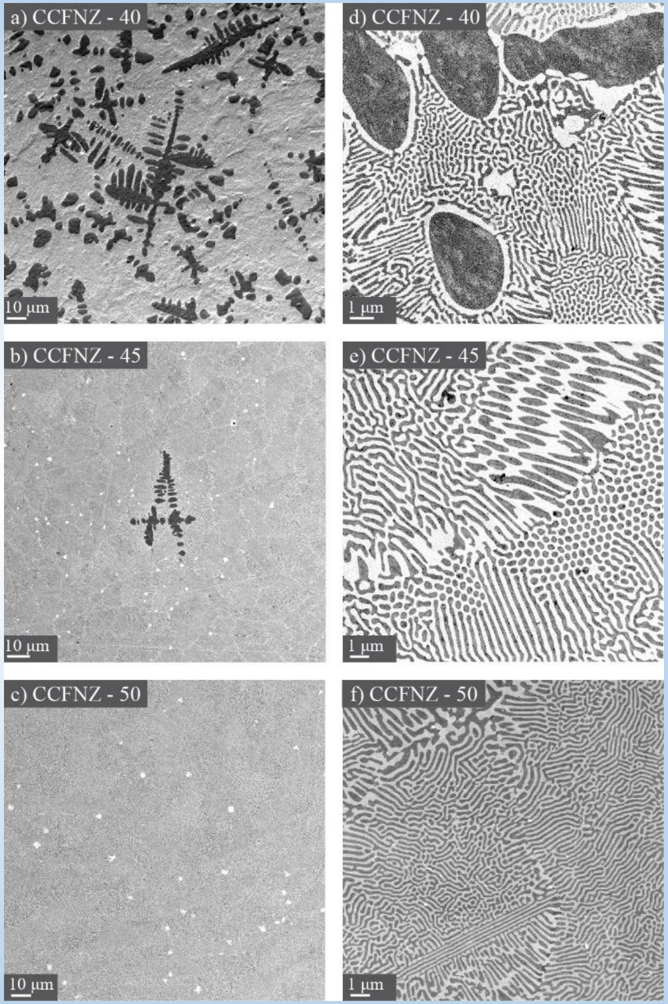

Examples of HEA systems

bcc and fcc HEAs:

Ta-Nb-Hf-Zr-Ti-Nb-Mo-V-W

Al-Si-Co-Cr-Cu-Fe-Mn-Ni-Ti

hexagonal HEAs:

Gd-Tb-Ho-Dy-Er-Tm-Lu-Y

- enhanced mechanical properties (high hardness, solid-solution strengthening)

- refractory materials (stable at high temperatures)

- superconductivity

- magnetic softness

- magnetic nanocomposites

- complex magnetic phase diagrams

Superconductivity in the Ta-Nb-Zr-Hf-Ti system

Ta-Nb-Zr-Hf-Ti:

9 % atomic radius mismatch between the largest (Zr) and the smallest (Ti) element

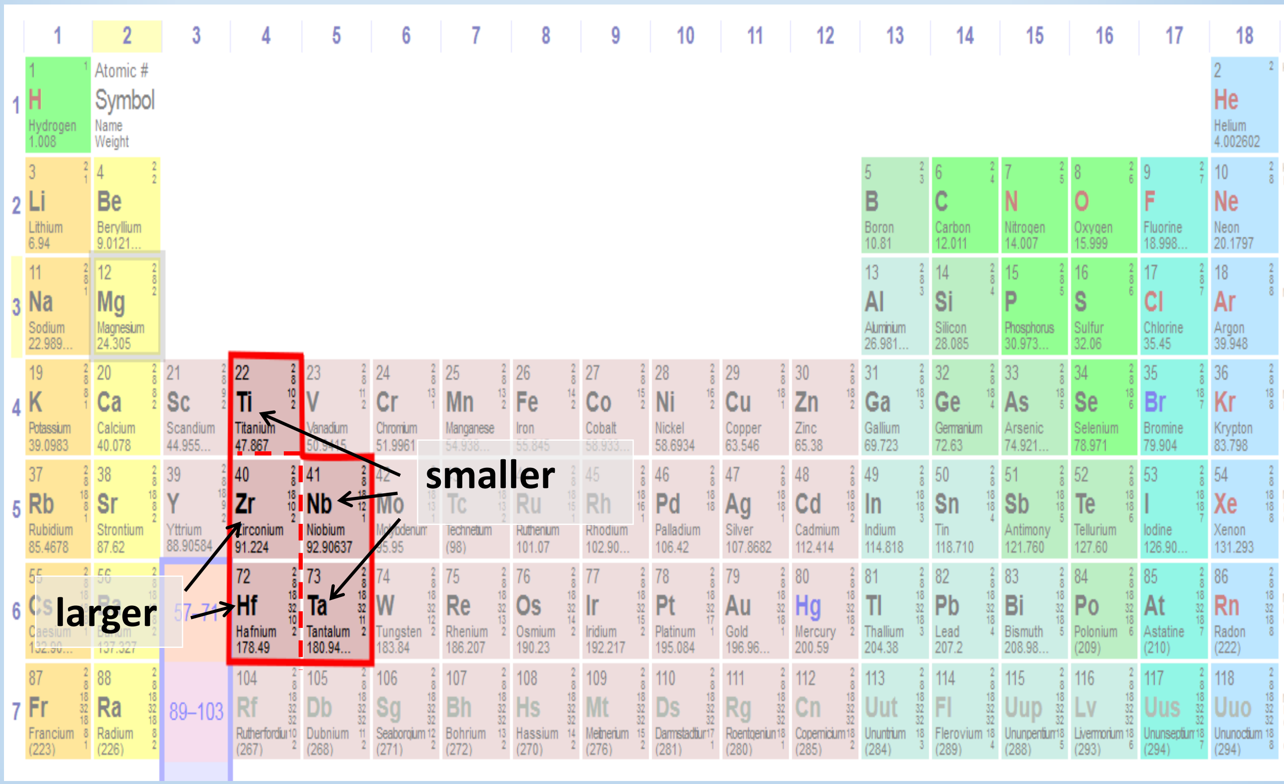

Superconductivity in the Ta-Nb-Zr-Hf-Ti system

Ta-Nb-Zr-Hf-Ti

electrical resistivity

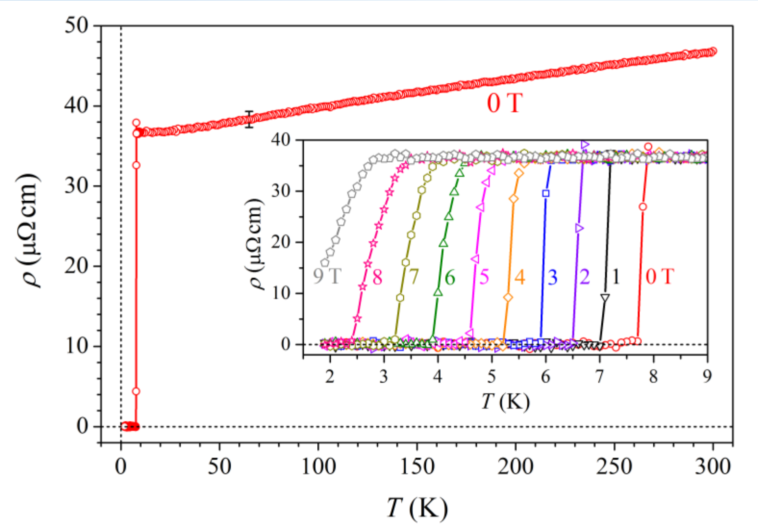

Meissner effect – type II superconductor

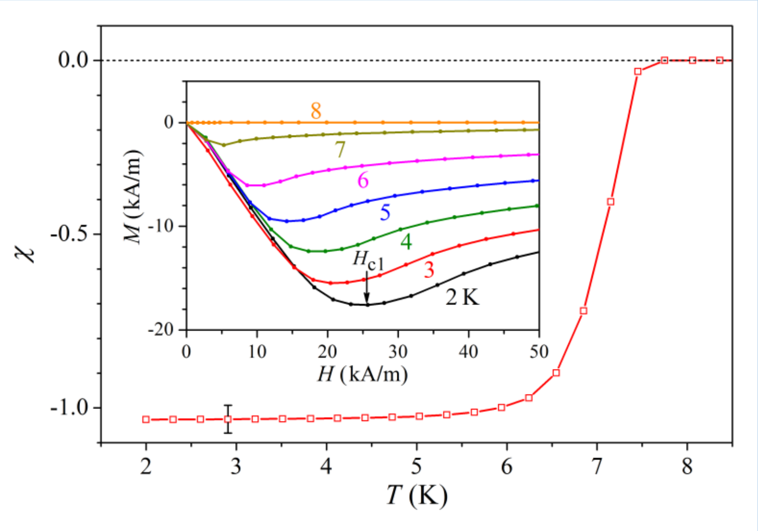

P. Koželj, *et al*., Phys. Rev. Lett. 113 (2014) 107001
S. Vrtnik, *et al*., J. Alloys. Compd. 695 (2017) 3530

Superconductivity in the Ta-Nb-Zr-Hf-Ti system

Ta-Nb-Zr-Hf-Ti specific heat

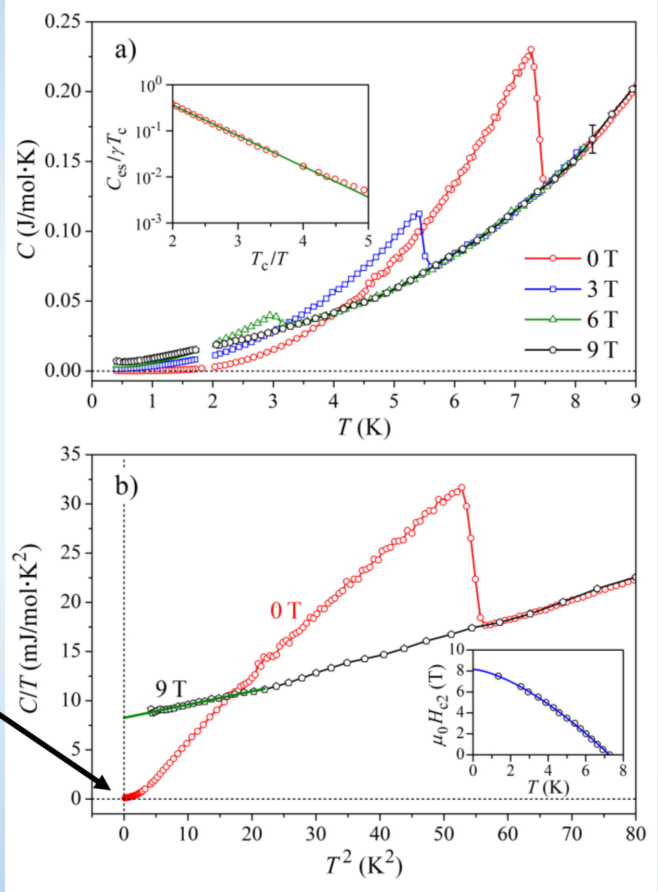

entire volume superconducting

Superconductivity in as-cast and thermally annealed Ta-Nb-Zr-Hf-Ti

$Ta_{34}Nb_{33}Hf_8Zr_{14}Ti_{11}$ zone melted

$Ta_{20}Nb_{21}Hf_{20}Zr_{20}Ti_{19}$ 7h@2000C

$Ta_{25}Nb_{25}Hf_{26}Zr_{24}$ 1day@1800C

$Ta_{22}Nb_{24}Hf_{21}Zr_{23}Ti_{10}$ 1day@1800C

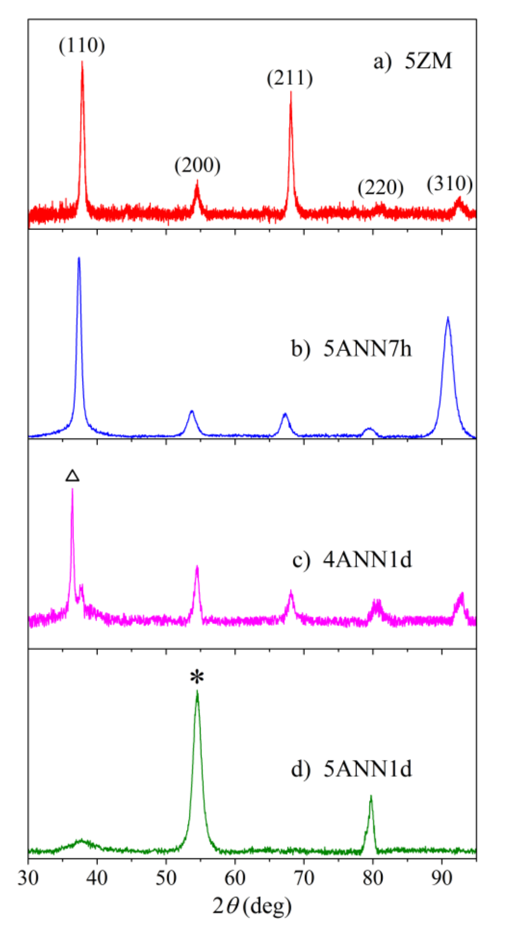

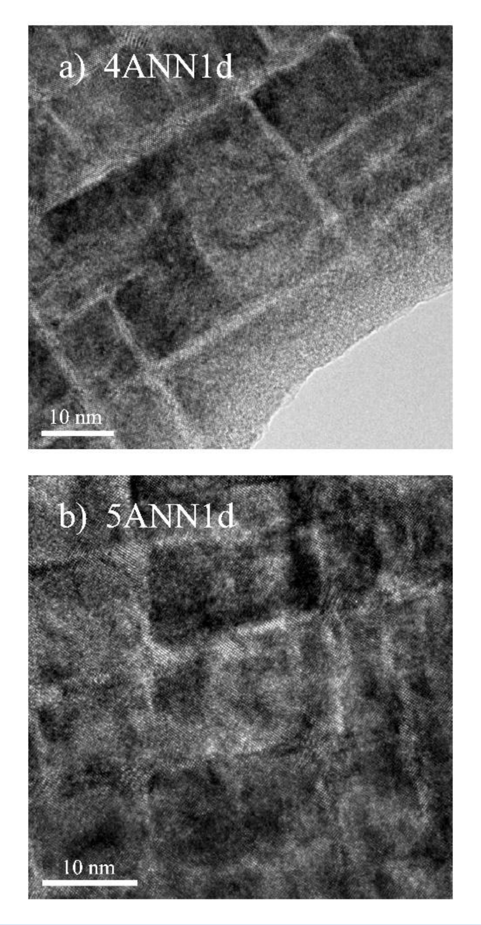

Superconductivity in as-cast and thermally annealed Ta-Nb-Zr-Hf-Ti

zero-field electrical resistivity

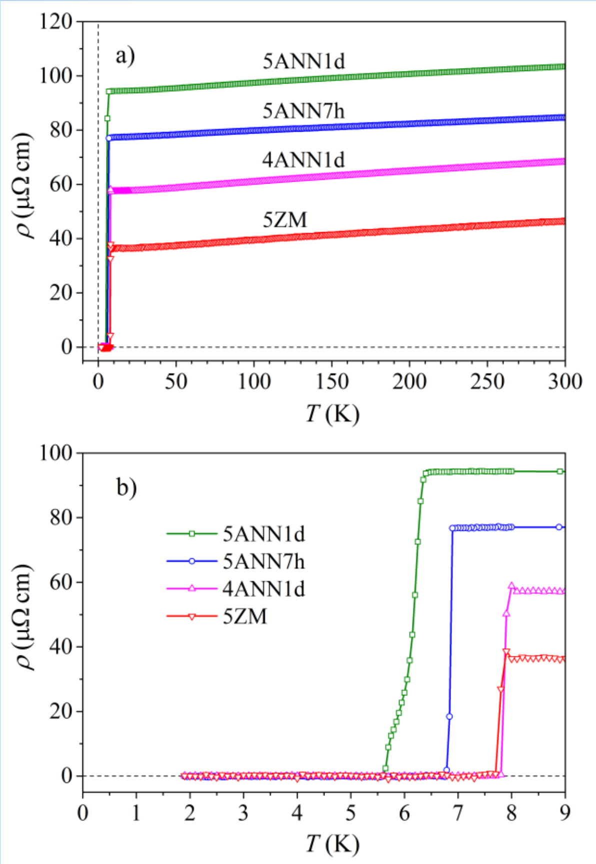

electrical resistivity in magnetic field

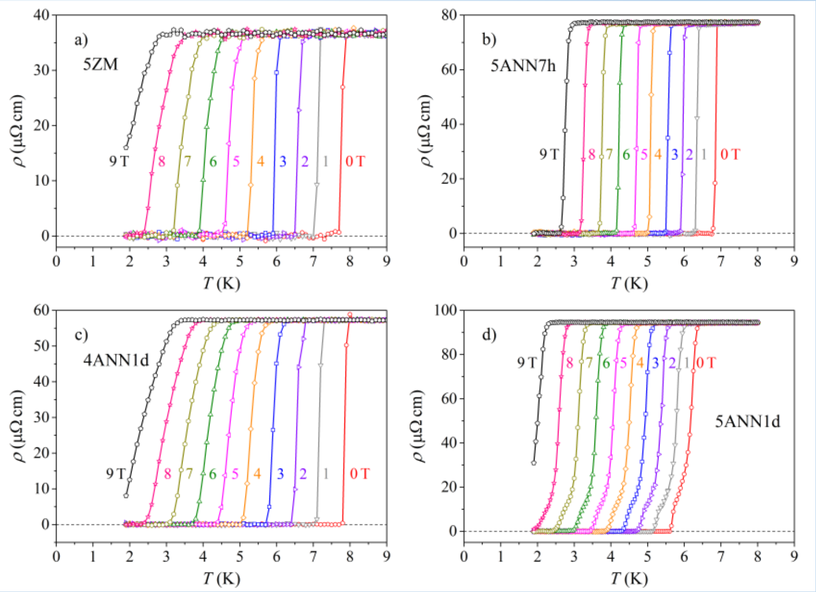

Superconductivity in as-cast and thermally annealed Ta-Nb-Zr-Hf-Ti

SC transition temperature – effect of structural inhomogeneity

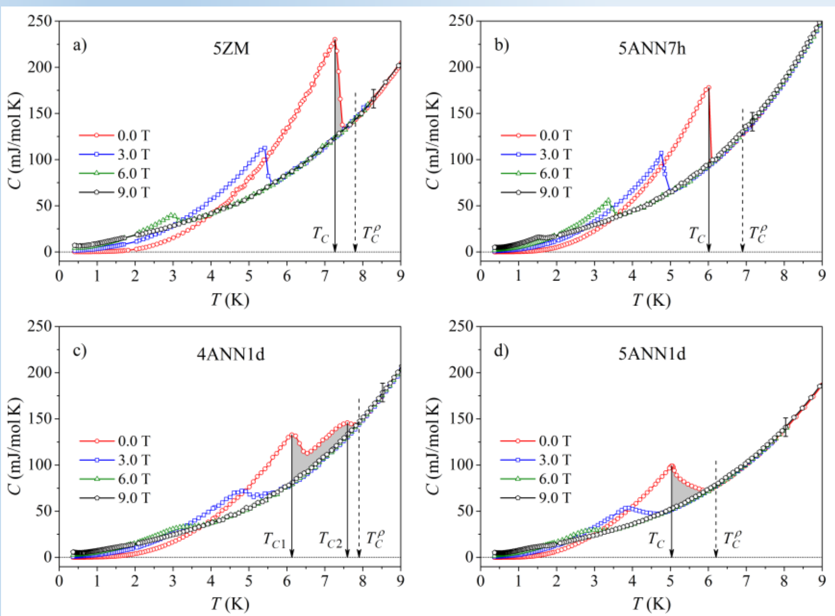

all samples are SC in the entire volumes, regardless of the composition and inhomogeneity

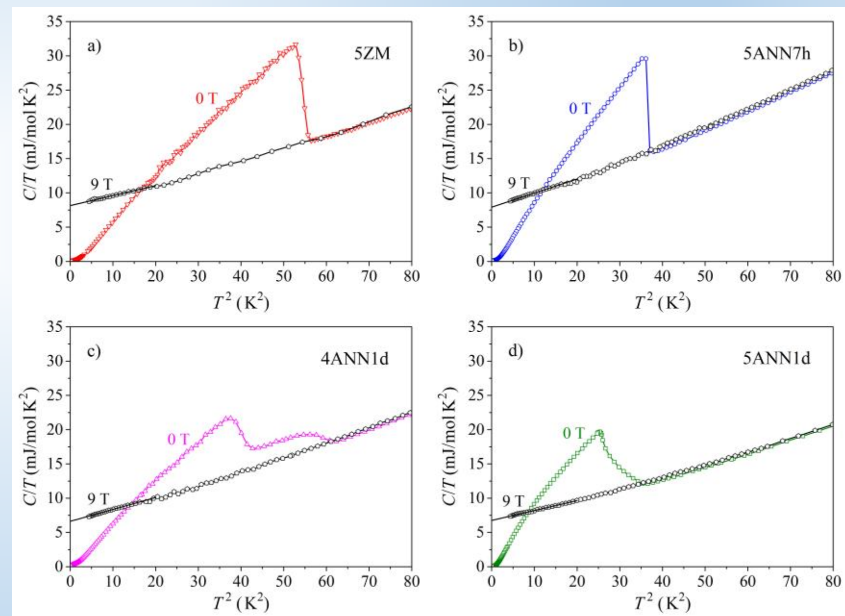

Superconductivity in as-cast and thermally annealed Ta-Nb-Zr-Hf-Ti

upper critical field

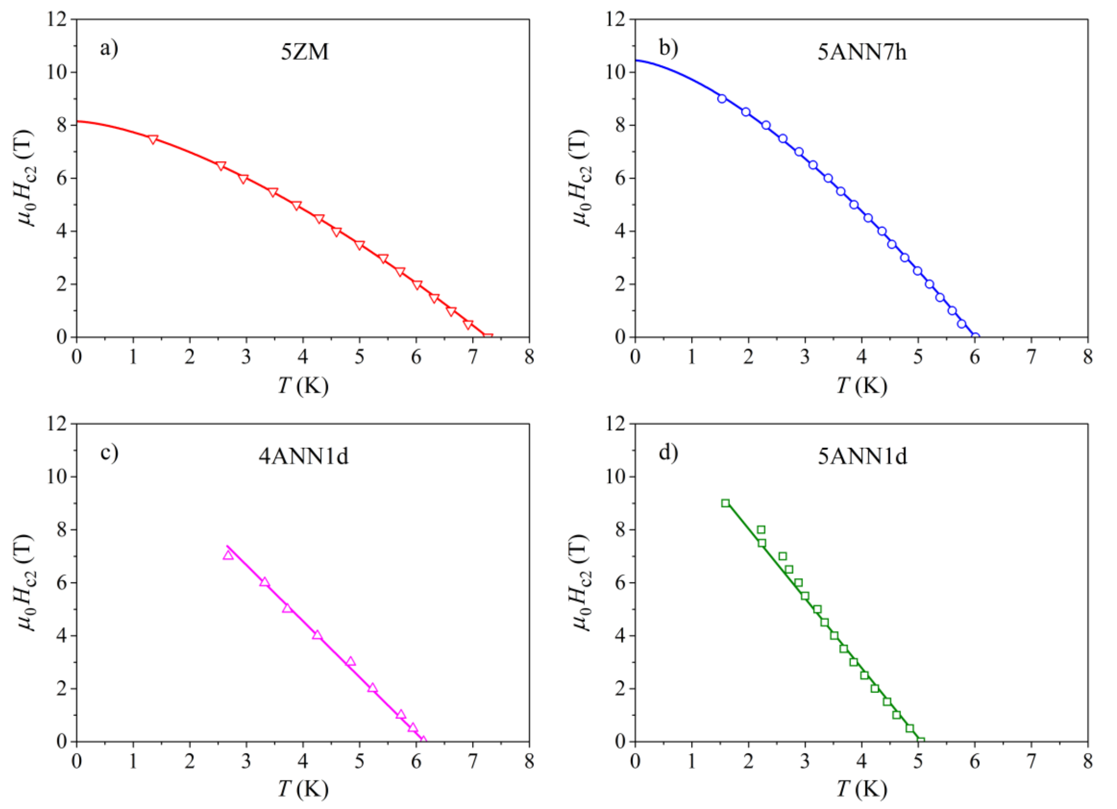

Soft ferromagnetism in FeCoNiPdCu

FCNPC: FeCoNiPdCu HEA
NES: non-oriented electrical steel ($Fe_{97}Si_3$)

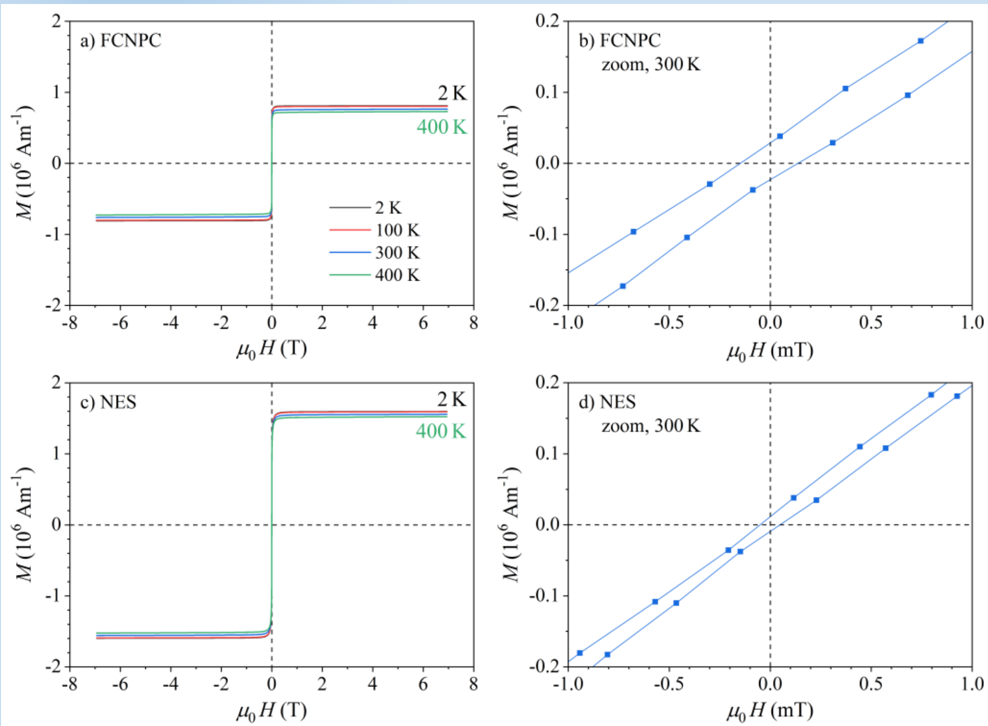

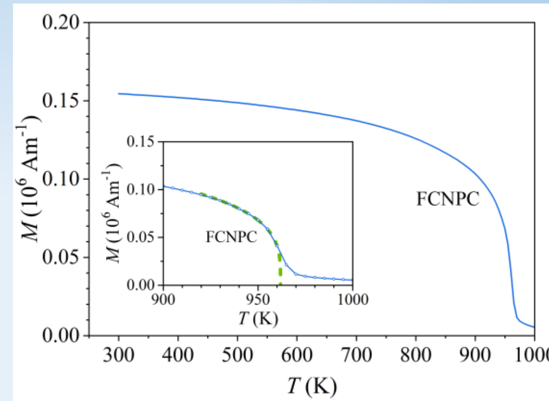

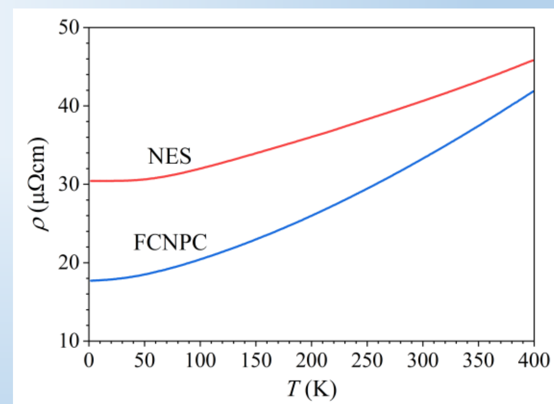

Use in: transformers, electromotors, electromagnetic machinery, magnetocaloric refrigerators

Soft ferromagnetism in FeCoNiPdCu

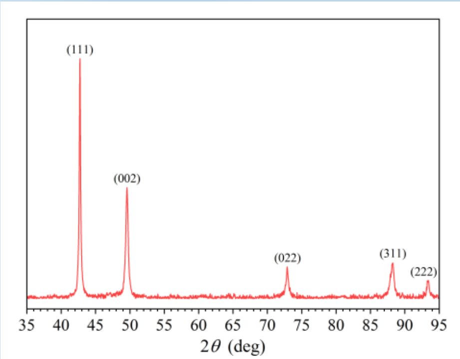

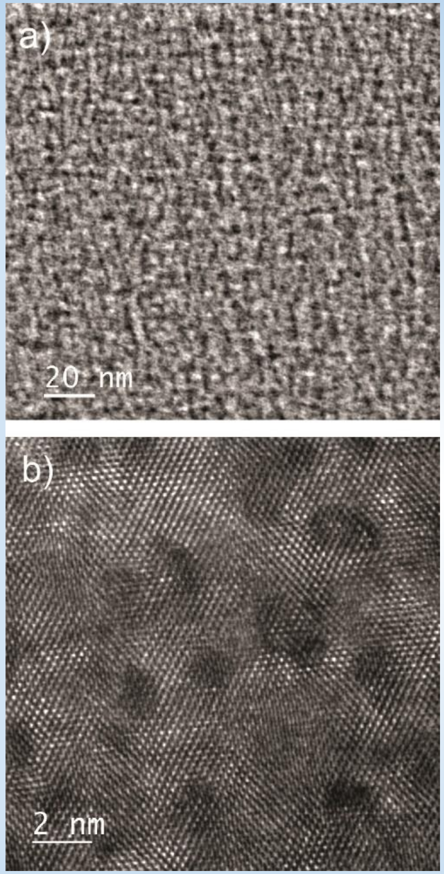

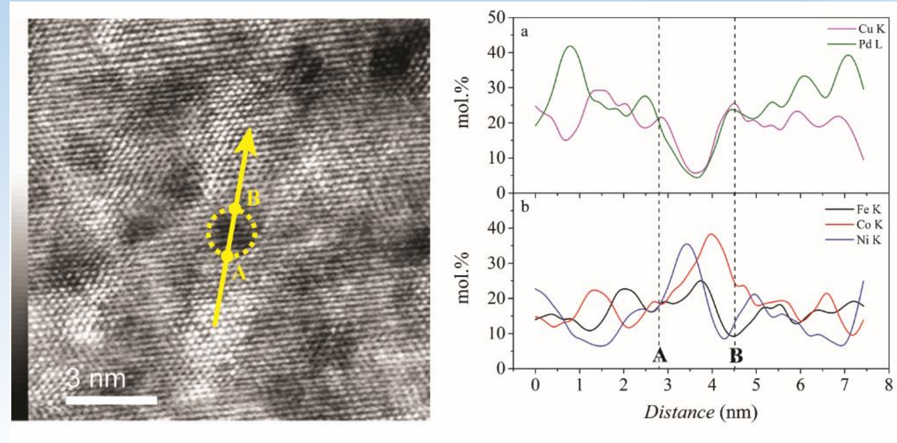

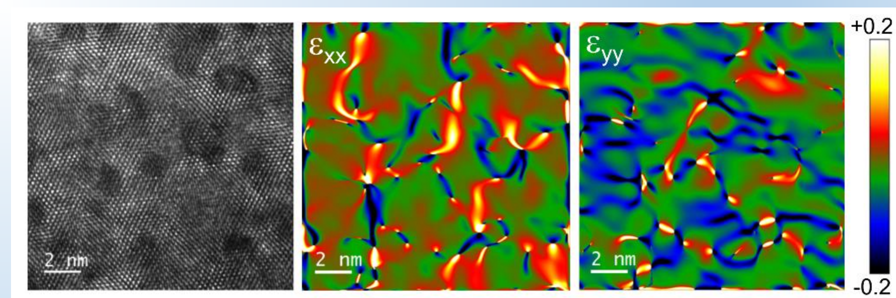

Nanocomposite of FeCoNi ferromagnetic nanodomains and CuPd nonmagnetic „nano-spacers“

→

exchange averaging of magnetic anisitropy

→

perfect magnetic softness

P. Koželj et al., Adv. Eng. Mater. (2019) 1801055
DOI: 10.1002/adem.201801055

Complex magnetism of rare-earth based hexagonal HEAs

- investigated system: Ce-Gd-Tb-Dy-Ho-Er-Tm-Lu
- binary mixing enthalpies of any pair of the elements are zero:

$$\Delta H_{mix}^{ij} = 0 \quad \Rightarrow \quad \Delta H_{mix} = 0 \quad \Rightarrow \quad \Delta G_{mix} = -T\Delta S_{mix}$$

- RE-based hexagonal HEAs are ideal solid solutions;

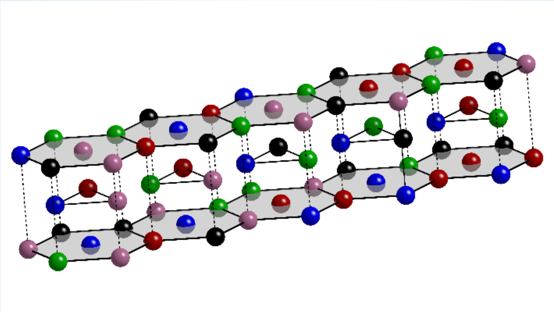

- atomic radii are very similar ⇒ lattice distortions small;
- large chemical disorder.

„Metallic glass on a topologically ordered lattice“

Physical properties of RE-based hexagonal HEAs

- Great chemical similarity of the RE elements ⇒ electronic properties can be predictably tuned with composition;

- Random mixing of RE elements on an undistorted hcp lattice results in unprecedented magnetic behavior;

- Complex (*H*,*T*) phase diagrams observed in Y-Gd-Tb-Dy-Ho [1] and Ce-Gd-Tb-Dy-Ho [2].

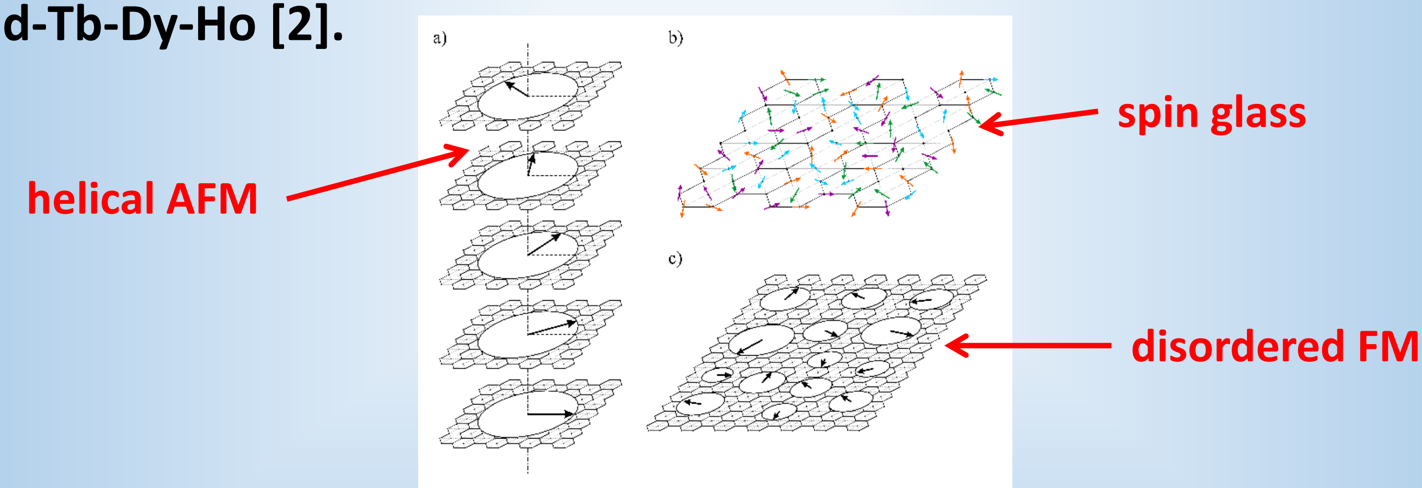

[1] J. Lužnik, *et al*., Phys. Rev. B 92 (2015) 224201.
[2] S. Vrtnik *et al*., J. Alloys Compd. 742 (2018) 877.

Physical properties of Tb-Dy-Ho-Er-Tm hexagonal HEA

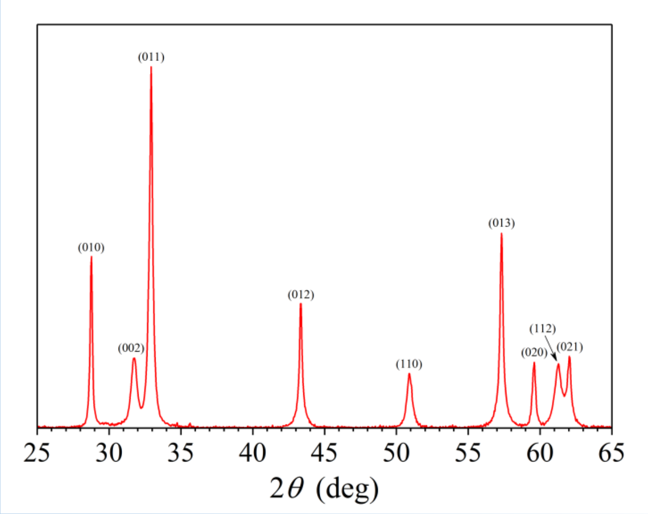

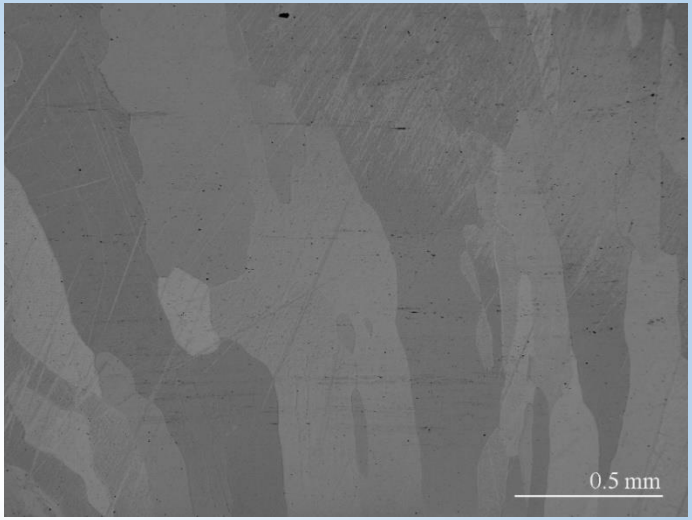

SEM BSE – channeling contrast

- single-phase material, macroscopically large grains;
- hcp structure, space group $P6_3/mmc$;
- RT lattice parameters: $a = 3.582$ Å and $c = 5.632$ Å, in good agreement with the composition-averaged theoretical values $\bar{a} = 3.575$ Å and $\bar{c} = 5.622$ Å;
- EDS composition: $Tb_{20.3}Dy_{20.7}Ho_{20.3}Er_{19.7}Tm_{19.0}$

Magnetic interactions in Tb-Dy-Ho-Er-Tm hexagonal HEA

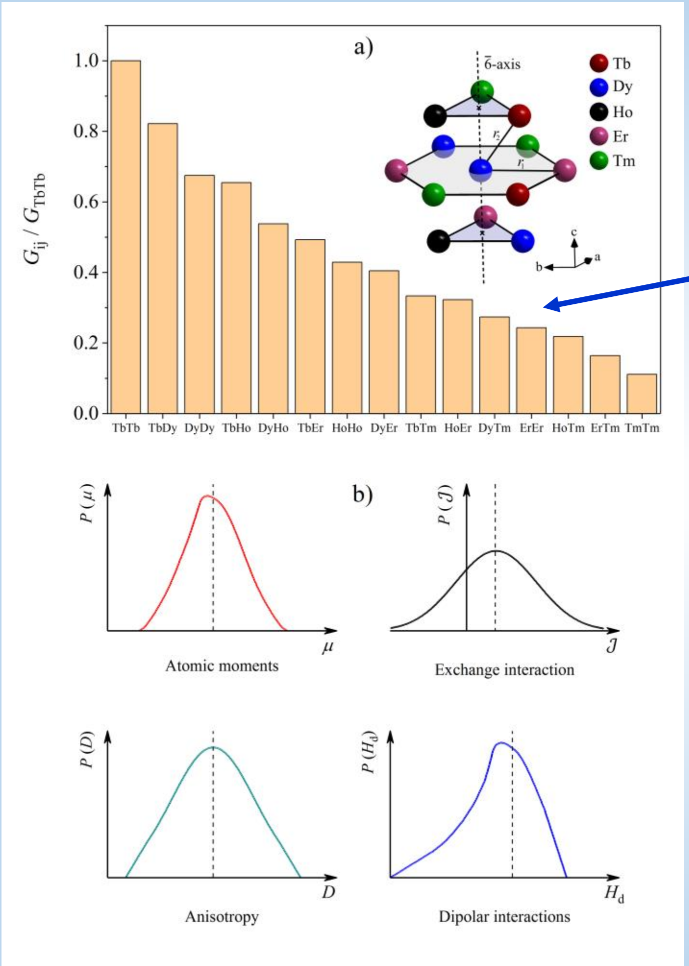

de Gennes factor (strength of the exchange interaction between different atomic pairs)

Probability distributions of:

- atomic magnetic moments $P(\mu)$,
- exchange interactions $P(\mathcal{J})$,
- magnetocrystalline anisotropy $P(D)$,
- dipolar interactions $P(H_d)$.

dc magnetization of Tb-Dy-Ho-Er-Tm hexagonal HEA

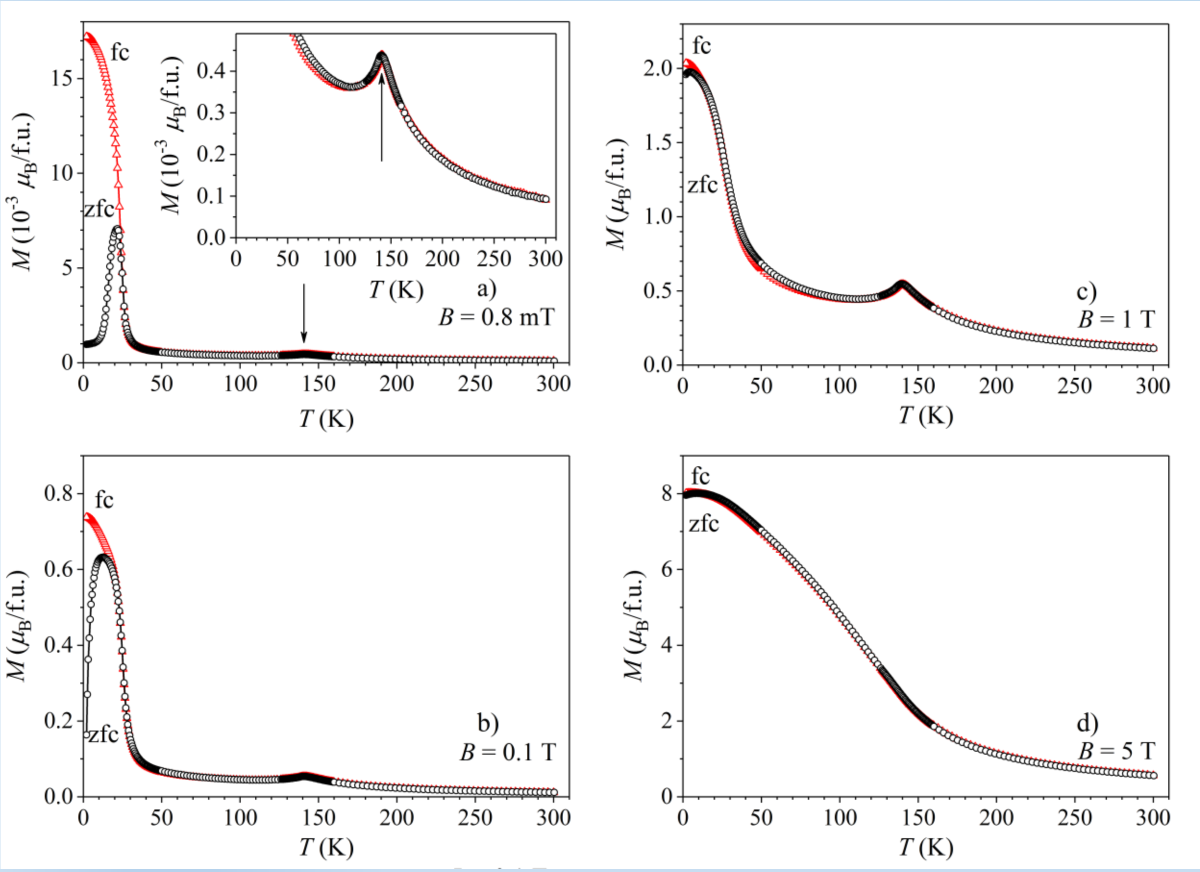

two magnetic phase transitions:

- **AFM-like at about 140 K**
- **FM-like at about 24 K**

ac magnetization of Tb-Dy-Ho-Er-Tm hexagonal HEA

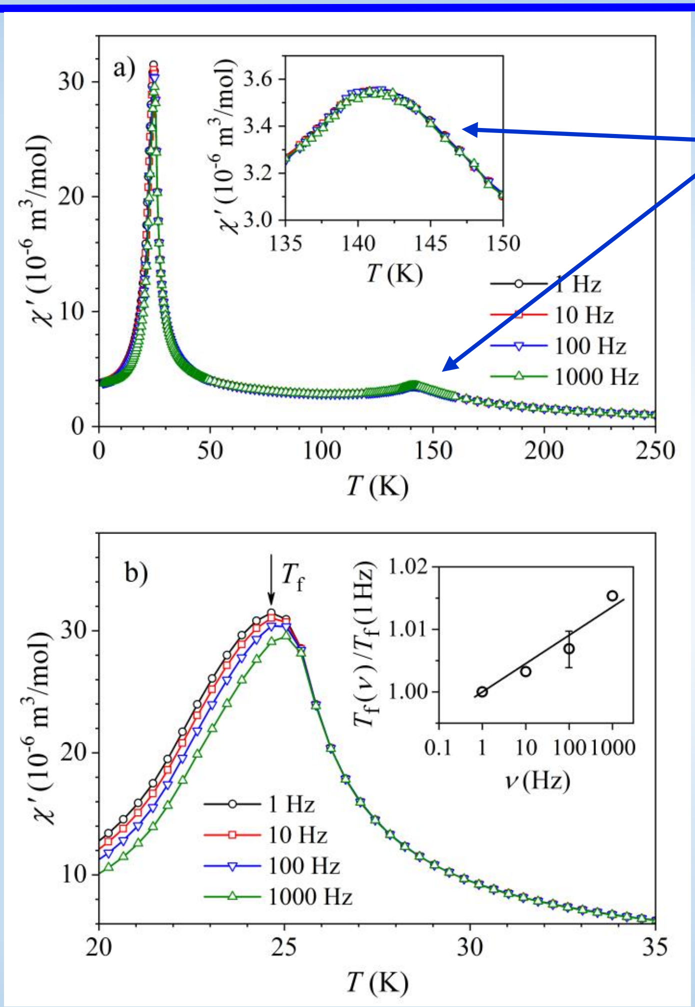

transition at 140 K is frequency-independent:

thermodynamic phase transition

transition at 24 K is frequency-dependent:

spin freezing transition in a magnetically frustrated system

M(H) curves of Tb-Dy-Ho-Er-Tm hexagonal HEA

M(H) dependence changes at a „critical“ field H_c

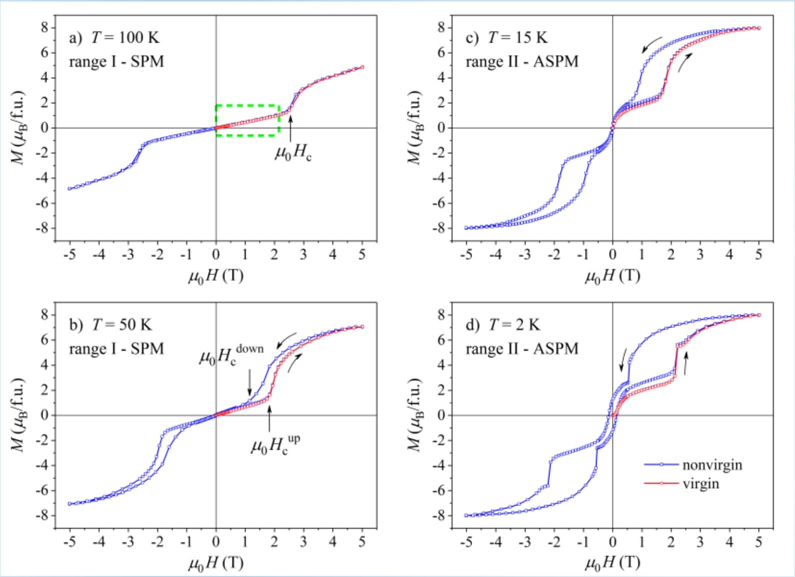

low-field M(H)

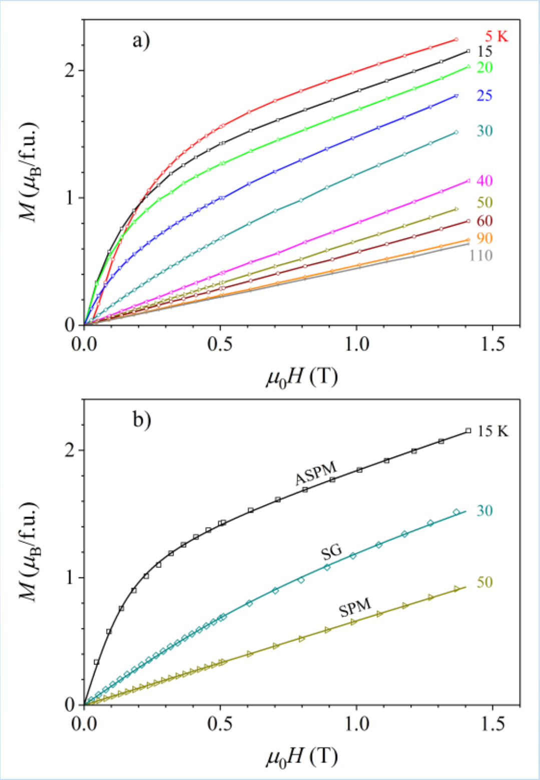

types of magnetic order

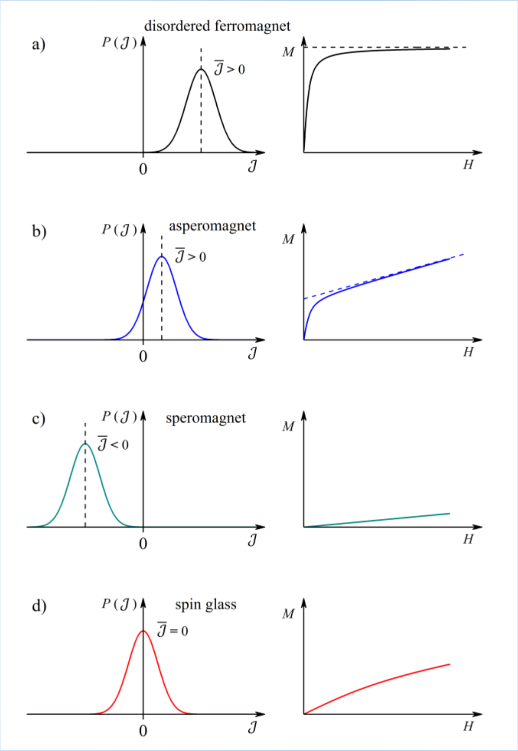

ASPM: asperomagnet

SPM: speromagnet

SG: spin glass

Thermoremanent magnetization time-decay of Tb-Dy-Ho-Er-Tm hexagonal HEA

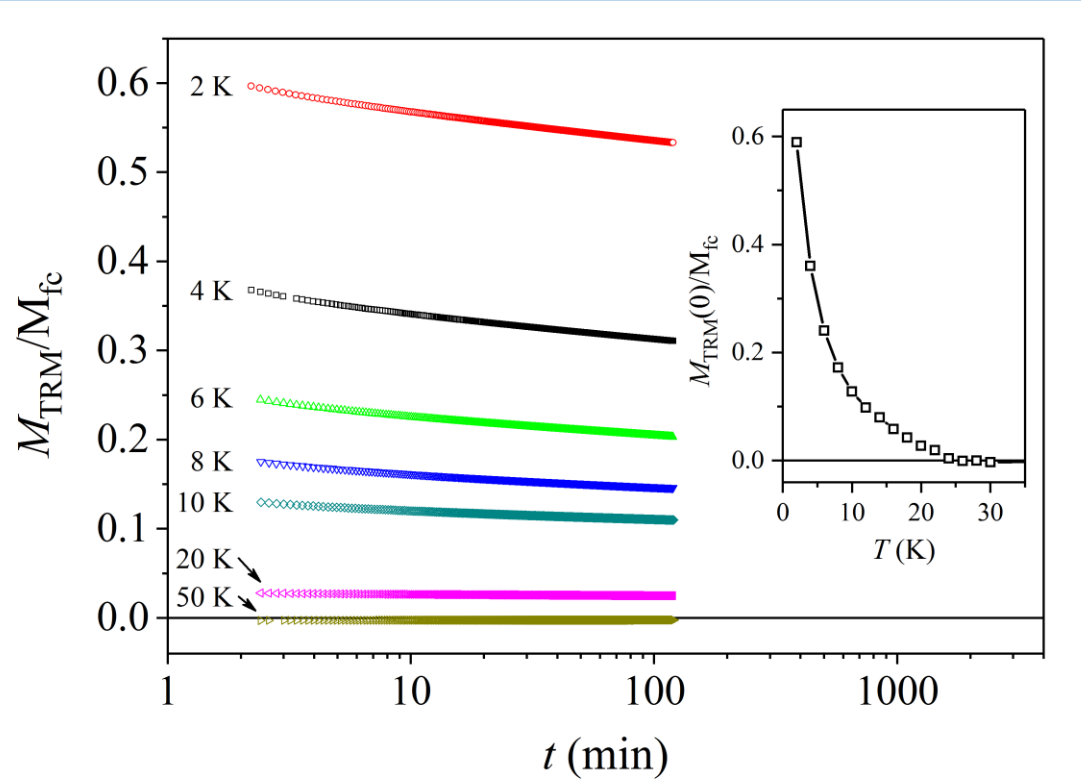

TRM is a measure of "stiffness" of the magnetically frustrated spin system, related to the length scale of the site-averaged magnetic moment correlations $\langle \vec{J}_i(0) \cdot \vec{J}_j(r) \rangle$.

FM correlations: large TRM; AFM correlations: small (or no) TRM

Specific heat of Tb-Dy-Ho-Er-Tm hexagonal HEA

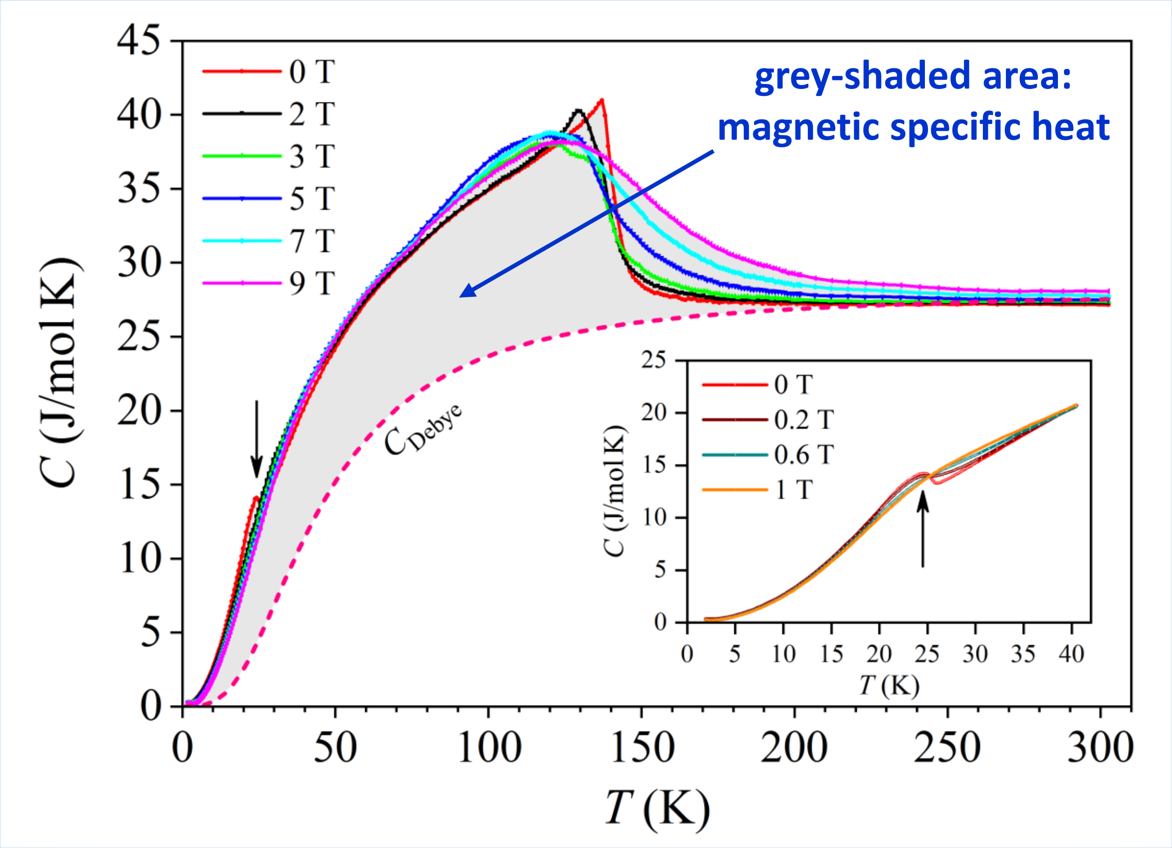

gradual magnetic ordering over a large temperature interval (200 – 2 K)

Electrical resistivity of Tb-Dy-Ho-Er-Tm hexagonal HEA

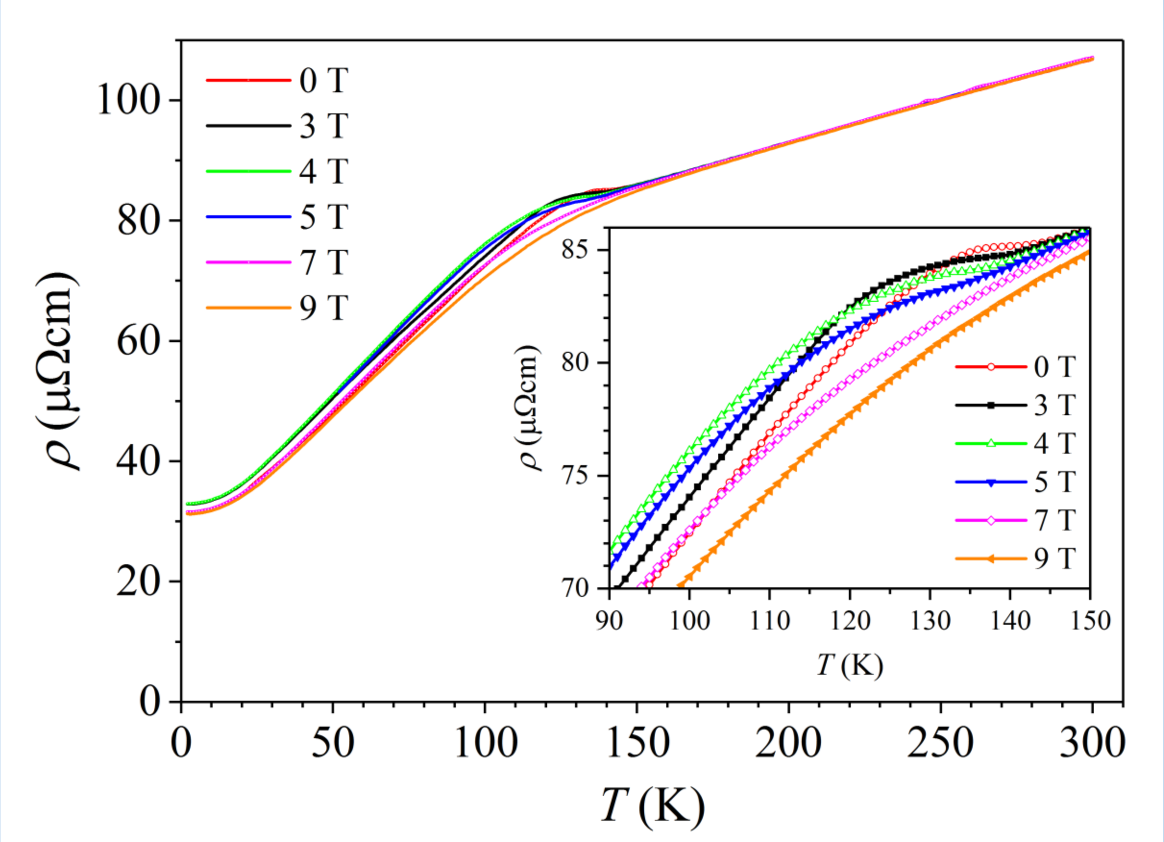

Magnetoresistance of Tb-Dy-Ho-Er-Tm hexagonal HEA

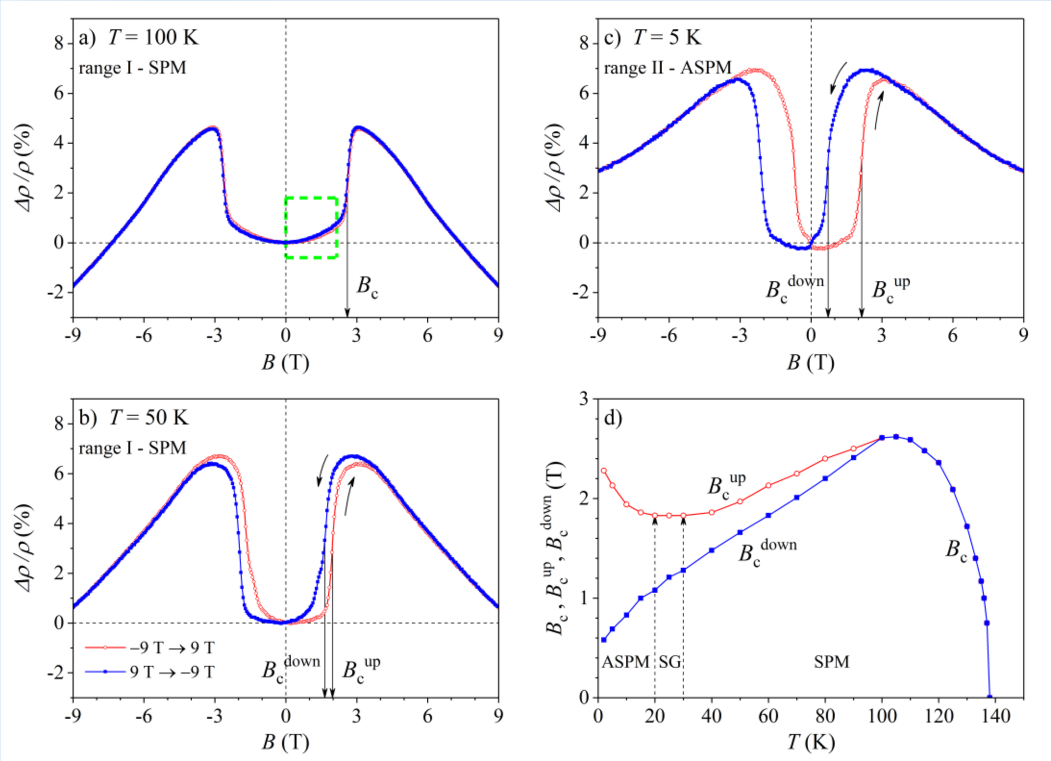

- magnetoresistance changes qualitatively at the critical field B_c;
- „up-down“ hysteresis of the critical field.

ANTIFERROMAGNET

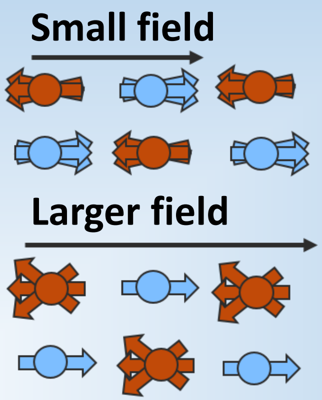

$\Delta\varrho/\varrho \propto B^2$

PARAMAGNET, FERROMAGNET

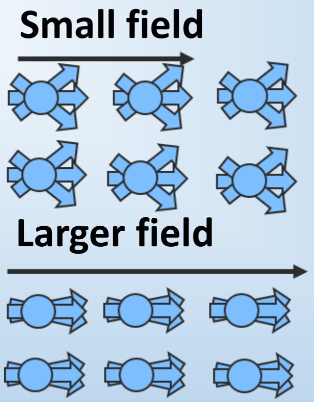

$\Delta\varrho/\varrho \propto -B$

Magnetic ground state of the Tb-Dy-Ho-Er-Tm hexagonal HEA

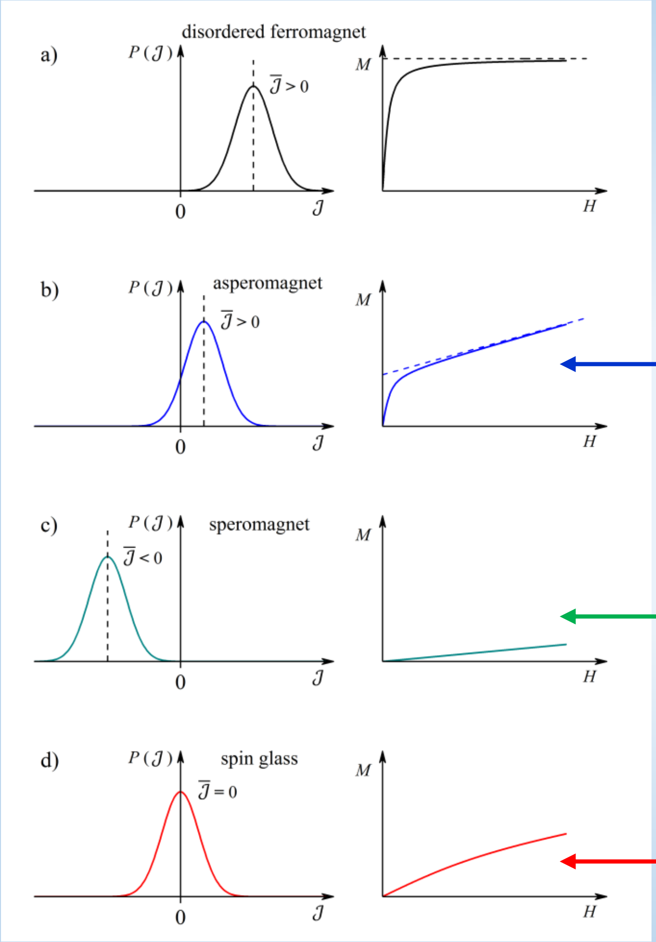

- asperomagnetic (disordered AFM) at high-T (between 140 and 30 K)
- speromagnetic (disordered FM) at low-T (below 25 K)
- must go through a spin glass state in the temperature range between 30 and 25 K

High-entropy alloys as novel functional materials

- superconductivity
- temporary (soft) magnets
- nanocomposite materials
- complex magnetic field-temperature phase diagrams
- magnetocalorics

Cooperation

Jožef Stefan Institute, Ljubljana

Stanislav Vrtnik
Janez Lužnik
Primož Koželj
Andreja Jelen
Jože Luzar
Mitja Krnel
Zvonko Jagličić
Anton Meden

Juelich research center, Juelich

Michael Feuerbacher

ETH Zuerich

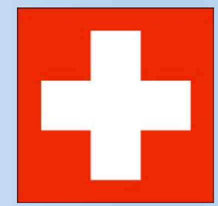

Walter Steurer
Soumyadipta Maiti

Origin of the ASPM ⟶ SG ⟶ SPM sequence of transitions

band structure effect, related to temperature-induced changes of the Fermi surface (analogy to pure heavy-RE metals)

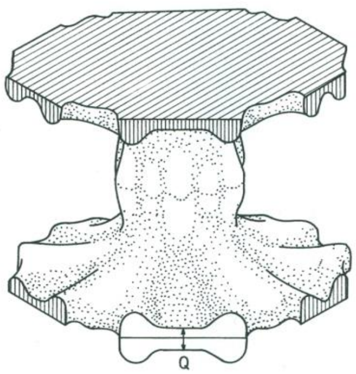

Fig. 1.11. The calculated hole Fermi surface of paramagnetic Tb in the Brillouin zone of Fig. 1.4. The extension of the 'webbing' between the 'toes' near the zone boundary is believed to give rise to a peak in the conduction-electron susceptibility $\chi(\mathbf{q})$, which determines the **Q**-vector characterizing the helical structure.

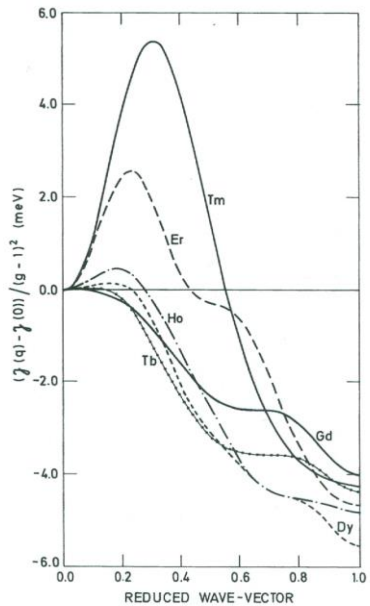

Fig. 1.17. The exchange interaction $\mathcal{J}_S(\mathbf{q}) - \mathcal{J}_S(\mathbf{0})$, determined experimentally in the magnetic heavy rare earth metals. The magnitude of the peak, which stabilizes the observed periodic magnetic structures, increases monotonically with atomic number.

J. Jensen, A.R. Mackintosh,
Rare Earth Magnetism
Clarendon Press, Oxford, 1991